JOURNAL OF APPLIED ELECTROCHEMISTRY **23** (1993) 1117–1124

Polarization and back e.m.f. in electrodialysis

S. J. JUDD, G. S. SOLT, T. WEN

School of Water Sciences, Cranfield Institute of Technology, Bedford, MK43 0AL, UK

Received 5 October 1992; revised 25 February 1993

Polarization and limiting current in electrodialysis (ED) are mass transfer phenomena usually described in terms of greatly rising electrical resistance of the depleted film. A simple and universally applicable technique has been developed to examine these. In actual operating conditions, direct measurement of the back electromotive force in a spirally wound electrodialysis (SPED) module suggests that the increase in ohmic resistance is minimal; the main mechanism is a large fall in the net e.m.f. From experimental results it is possible to evaluate membrane surface concentrations and hydrodynamic boundary layer thickness directly.

List of symbols

C	concentration (M)
C	concentrate/diluate concentration ratio
C^*	surface concentration, (M)
D	diffusion coefficient ($m^2 s^{-1}$)
E_b	back e.m.f in a cell pair, (V)
F	Faraday constant ($C mol^{-1}$)
I_{lim}	limiting current density ($A m^{-2}$)
n	change in charge number in electrode reaction
R	gas constant ($J K^{-1} mol^{-1}$)
t	elapsed depolarization time (s)
t	elapsed polarization time in Equation 12 (s)
T_s, T_m	solution, membrane transport number
T	absolute temperature (K)
V	applied voltage across module (V)
w	quantity of diffusing species ($mol m^{-2}$)
x	distance from membrane surface (m)
γ	activity coefficient
δ	thickness of the boundary layer (m)
τ	relaxation time (s)

Subscripts

1	diluate
2	concentrate

1. Introduction

Electrochemical polarization describes a set of phenomena which arise when a current passes across an interface at a current density which is greater than that which the interface will transmit under kinetically-limited conditions. For an electrodialysis (ED) process, polarization at the ion-exchange membrane/solution interface takes place when permeation of the electrically-transported ion through the membrane is faster than diffusion transport of the ion to the membrane surface. Beyond the critical point, the surface concentration of the transported ion is zero, and ion transport becomes diffusion limited. This condition manifests itself in the form of a sharp increase in the apparent resistance of the cell.

Many reports concerning concentration polarization and membrane potential (or *back* e.m.f.) in ED systems have been published over last 50 years [1–10]. In predicting or demonstrating these mass transfer phenomena, past investigations have generally been carried out in specially designed cells, which are subject to at least one of the following constraints: (i) a small membrane area (i.e. a few cm^2) [3, 6, 8–10], (ii) a large cell thickness (i.e. more than 10 mm) [3, 7], and (iii) an unrealistic time period (40–150 ms) for capturing relaxation data [2, 3, 8, 9].

The investigation of a small sample of membrane (i) ignores physicochemical heterogeneities existing throughout a complete stack system, whilst employing a larger than normal cell thickness (ii) alters the process hydrodynamics. Conversely, results from empirical studies of a complete stack represent only a composite picture of the range of conditions within it, and therefore cannot be used to predict the process performance under differing operating conditions.

The direct measurement of the voltage transient during relaxation (iii) has received little attention, although early studies using oscilloscopes to capture data have been reported [2, 3]. Relaxation of the depleted region adjacent to the membrane surface on the diluate side would be expected to take place when the operating voltage across the cell is stepped down to zero. A voltage decay curve would then be produced by depolarization of the concentration boundary layer, reducing the concentration differential across the membrane.

Few studies of relaxation in ED systems have been carried out previously and [8, 9] have failed to detect the expected voltage decay, due to the delay in the capturing of data (approximately 40 ms) following the zeroing of the applied voltage. The equilibrium back e.m.f. is given by the bulk concentration values according to the Nernst equation:

$$E_b = \frac{2RT}{nF}\log\left(\frac{C_2\gamma_2}{C_1\gamma_1}\right) \qquad (1)$$

per cell pair, where C_2 and γ_2 are the respective bulk concentration and activity coefficient values of the concentrate and C_1 and γ_1 the equivalent values for the diluate.

In NaCl solution, at 298 K, with the value of R as $8.314\,\mathrm{J\,K^{-1}\,mol^{-1}}$ and F as $96\,500\,\mathrm{C\,mol^{-1}}$, assuming activity coefficients γ_1 and γ_2 of unity, Equation 1 becomes:

$$E_b = 2 \times 0.05913\ \log\left(\frac{C_2}{C_1}\right) \qquad (2)$$

In the current paper, results from the instantaneous measurement of the back e.m.f. are presented. The voltage decay was measured from the instant the applied voltage was stepped to zero using the novel SPED module [11]. The paper follows on from results previously presented for a mathematical model describing desalination by the SPED apparatus [12].

2. The spirally-wound module: previous work

The work reported here is incidental to the development of a spirally-wound (SPED) module, in which two spiral cells are created, so that both concentrate and diluate streams flow in long spiral paths (Fig. 1). This allows large desalting ranges to be achieved in a small apparatus, in contrast to conventional stacks. A description of the module has been given in previous publications [11–13]. It's most striking feature is the long cell path, which yields a significant change in concentration from core to shell.

The spiral module is ideally-suited for back e.m.f. studies: as there is only one cell pair, the hydraulic and concentration conditions are known throughout, and in the absence of electrical leakage paths reliable measurement is possible.

A mathematical model describing desalination in a SPED module has been developed, yielding a computer model which can predict the complex dimensional, electrical, chemical and hydraulic relationships in spiral parallel flow [12]. The model was originally designed to predict the module performance under non-polarizing conditions, i.e. assuming the back e.m.f. to be given by the difference in bulk concentration of the solutions in the apparatus using Equation 2.

Actual modules have been designed and fabricated on the basis on the computed predictions. Apparatus, experimental procedures and results from the operation of these modules have been presented [13]. It has been demonstrated that the model predicts actual operational parameter values with reasonable accuracy, the exception being the operating voltage. The predicted values for this parameter are much lower, and this can clearly be attributed to concentration polarization, which is not taken into account by the model but is to be expected under the conditions stipulated [14].

3. Polarization and the concentration boundary layer

The back e.m.f. generated by concentration polarization is given by the Nernst expression:

$$E_b = 0.118\ \log\left(\frac{C_2^*}{C_1^*}\right) \qquad (3)$$

per cell pair, where C^* refers to the solution concentration at the membrane/solution interface. Under conditions of complete polarization, there is no theoretical lower limit for C_1^*, such that E_b can become very large.

According to the idealized Nernstian model of the boundary layer, the change in concentration between the bulk liquid and the membrane surface is envisaged as taking place within the semi-stagnant layer of liquid next to the membrane surface, the hydrodynamic boundary layer. The thickness of this layer, δ, is determined by the system hydrodynamics, decreasing with increasing fluid turbulence. Since it is a characteristic of an idealized system, in which the liquid within the boundary layer is considered to be stagnant, its value in any practical apparatus cannot be predicted from hydrodynamic data alone.

The diffusion limited current density can be derived from the Nernst–Planck equation, and is related to δ by the following equation:

$$I_{\mathrm{lim}} = \frac{nFDC_1}{\delta(T_m - T_s)} \qquad (4)$$

where D is the diffusion coefficient, and T_m and T_s are the ion transport numbers in the membrane and

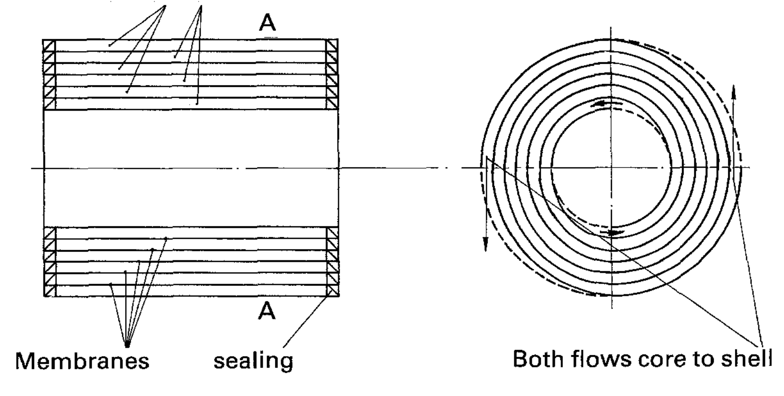

Fig. 1. SPED module.

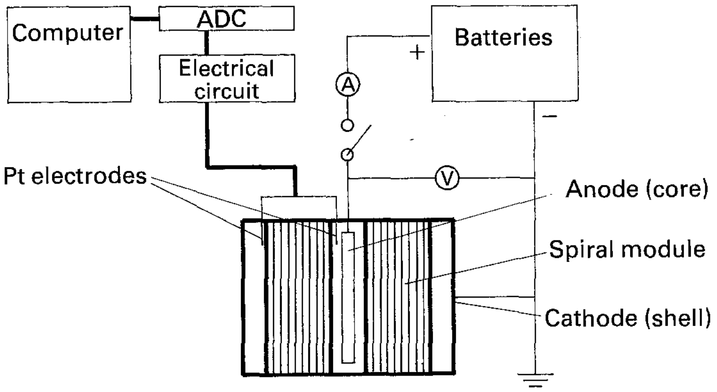

Fig. 2. Data acquisition system.

solution respectively. I_{lim} can be measured directly, provided the onset of polarization is identified.

The relationship between δ and τ, the relaxation time, can be obtained directly from Fick's law. Accordingly, the quantity of electrolyte $\mathrm{d}w$ diffusing across 1 m^2 in time $\mathrm{d}t$ when the concentration gradient is $-\mathrm{d}c/\mathrm{d}x$ is

$$\mathrm{d}w = D\left(\frac{\mathrm{d}c}{\mathrm{d}x}\right)\mathrm{d}t \tag{5}$$

where D is the diffusion coefficient.

If the concentration change within the boundary layer is regarded as being uniformly linear during polarization [20], then, for a stagnant film, the total quantity w (per m^2) diffusing from the bulk to the boundary layer for complete depolarization is

$$w = C\delta/2 \tag{6}$$

where C is the bulk concentration.

The concentration gradient $\mathrm{d}c/\mathrm{d}x$ is C/δ at $t = 0$, and drops to 0 at $t = \tau$, t being the elapsed depolarization time. Integration of Equation 5 from time 0 to τ gives

$$w = DC\tau/2\delta \tag{7}$$

Hence, from Equations 6 and 7,

$$\delta = (D\tau)^{1/2} \tag{8}$$

If τ can be determined directly, then the approximate thickness of the layer δ may be calculated by Equation 8.

4. Experimental details

4.1. *Data acquisition system*

The data acquisition system used for multiple electrode voltage measurement is schematically presented in Fig. 2. Essential features of the apparatus are as follows:

(i) An electronic circuit, which reduces the voltage signals from the module by a factor of five.
(ii) A 16 channel analog to digital converter (ADC) which converts the voltage signals to integers in the range 0 to 4095.
(iii) A personal computer, which was used to set electrode scanning rate and sampling frequencies and to produce data files which could be used for analysis and manipulation.

The electronic circuit (i) was incorporated to provide a compatible input voltage to the ADC (which has a capacity of 10 V compared with a maximum voltage drop of about 42 V across the module). Voltages were recorded at a speed of 800 Hz, and the system calibrated using a digital multimeter and oscilloscope.

4.2. *Experimental procedure*

A 14-turn spirally-wound ED module was used. The dimensional data of the spiral module and hydrodynamic data of the experiment are presented in Table 1.

Table 1. Experimental conditions

SPED module dimensions					
Cell length:	7.7 m	Height:	200 mm	Inner dia.:	130 mm
Cell area:	1.54 m^2	Turns:	14	Outer dia.:	220 mm
Anion membrane					
Thickness:	0.6 mm	Resistance:	$< 10\,\Omega\,\mathrm{cm}^{-2}$	Selectivity:	> 0.92
Cation membrane					
Thickness:	0.6 mm	Resistance:	$< 8\,\Omega\,\mathrm{cm}^{-2}$	Selectivity:	> 0.94
Diluate cell					
Inlet:	81.9 mM	Thickness:	1.2 mm	Porosity:	0.89
Outlet:	8.9 mM	Velocity:	100 $\mathrm{mm\,s}^{-1}$	*Re* number:	148
Concentrate cell					
Inlet:	81.9 mM	Thickness:	0.6 mm	Porosity:	0.94
Outlet:	314.0 mM	Velocity:	60 $\mathrm{mm\,s}^{-1}$	*Re* number:	55

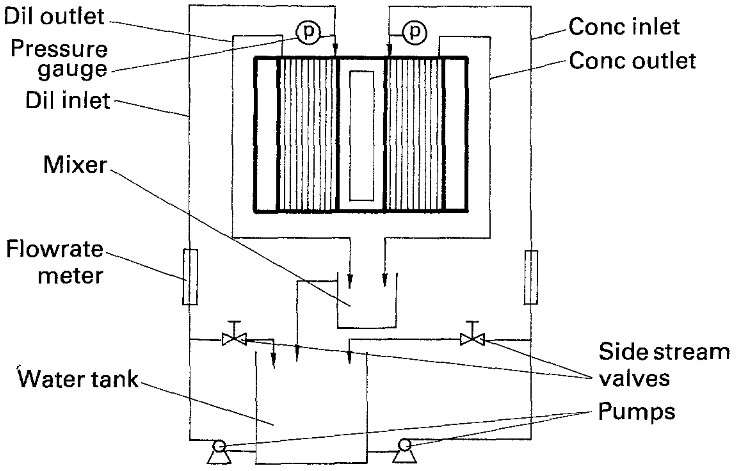

Fig. 3. Flow system.

Figure 3 shows the flow system. Feed solution was introduced to core inlets of the concentrate and diluate compartments of the SPED module. Samples of the diluate and concentrate were taken at their respective outlets prior to combining and mixing the two streams and returning the solution to the inlet tank.

A set of lead : lead oxide acid batteries were used to provide a stable d.c. current. The applied voltage ranged from 6 to 54 V, with increments of 6 V. Electrical current and voltage were measured using digital multimeters.

Electrical voltage data were obtained from 16 Pt electrical probes (diameter = 0.25 mm, length > 50 mm) in the module, which were planted in every cell pair, core and shell, and connected to the data acquisition system. The module voltage changes were measured by the probes planted at the core and shell respectively, as shown in Fig. 2.

After the hydraulic condition was adjusted to the required values, the external e.m.f. was maintained for about 30 min to obtain stable conditions. On stabilizing the hydraulic system, the computer program was initiated to record module relaxation voltage data at a speed of 800 Hz, i.e. one reading every 1.25 ms, immediately following the zeroing of the external e.m.f. Data were recorded for approximately 1.2 s.

5. Results and discussions

5.1. *Back e.m.f. and membrane surface concentration*

Figure 4 shows a typical voltage transient for the SPED module, obtained under conditions of concentration polarization (applied voltage, $V = 33.4$ V). Zero time has been set at the point at which the last applied voltage was recorded. This figure includes data obtained from a comparative experiment in which the external e.m.f. was not connected to the SPED apparatus (represented by empty squares). Under these conditions the recorded voltage drops from a steady level of 36.0 to 0 V after one interval (1.25 ms).

The solid triangles represent experimental data from the SPED module: the recorded e.m.f. readings fall from the applied voltage value of 33.4 to 22.4 V within 1.25 ms. The voltage readings then fall steadily for about 9 ms, to a reading of 12.8 V, and then fall sharply to 2.65 V. This last value represents the concentration potential due to the bulk liquids according to Equation 2, and corresponds closely to the value predicted by the model. A further slow fall in the e.m.f. readings over an extended time period (i.e. several hours) reflects slow equalization of the two solutions by osmosis and ionic diffusion.

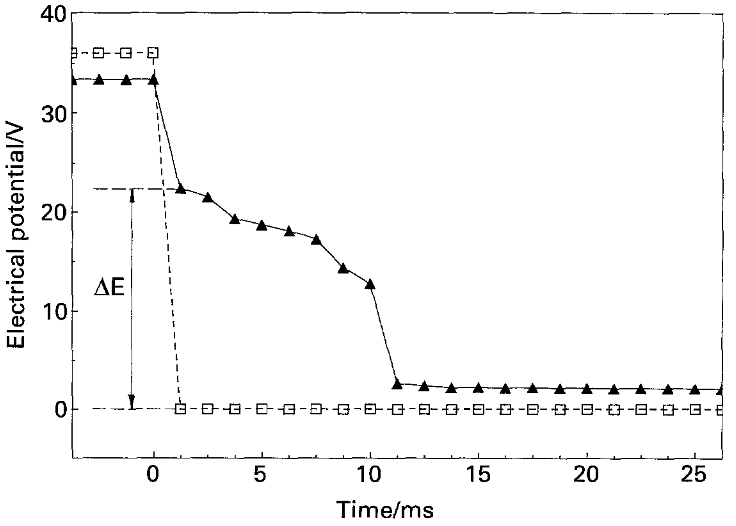

Fig. 4. Voltage (depolarization) transients. Operating parameters given in Tables 1 and 2. Key: (–□–) Blank, (–▲–) sample.

Table 2. Comparison of experimental results with computer model

Parameter	*Computer model*	*Experimental data*
Current (A)	13.0	12.9
Total applied e.m.f. (V)	12.8	33.4
Back e.m.f. (V), from bulk concentration	2.3	2.4
Operational back e.m.f. (V)	2.3	22.4
Effective e.m.f. (V)	10.5	11.0
Dil. pressure (bar)	0.72	0.75
Conc. pressure (bar)	0.59	0.65
Dil. and Conc. inlet (mol m^{-3})	81.9*	81.9
Dil. outlet (mol m^{-3})	8.9*	8.9
Conc. outlet (mol m^{-3})	339.4	314.0

* Experimental data used for computational analysis

Table 2 compares experimental results with the computer prediction. According to the data shown, the discrepancy of some 20 V between the predicted operating voltage and the experimental voltage corresponds very closely to the recorded total voltage decay ΔE shown in Fig. 4. The results strongly suggest that the recorded voltage decay ΔE is the back e.m.f. It is suggested that this parameter is principally responsible for limiting the operational efficiency of the ED process, rather than the increase in ohmic resistance of the diluate.

The maximum back e.m.f. recorded was about 3.0 V per cell pair at the shell of the module, where the bulk concentration difference (8.91 mM and 314.0 mM for the diluate and concentrate respectively) is at its greatest. According to Equation 3, the back e.m.f. suggests a trans-membrane concentration ratio C_2^*/C_1^* of approximately 10^{25}, considerably more than the bulk concentration ratio of 35. The maximum possible C_2^* value is constrained by the NaCl solubility of 6 M [17], suggesting that the interfacial diluate concentration is of the order of about 10^{-24} M. Clearly, such a concentration and the resulting back e.m.f. impose a severe restriction on the operational efficiency of the process.

It should be pointed out that the Nernst equation is thermodynamic in origin, i.e. depends on a meaningful value of chemical potential (an equilibrium quantity) being definable in a statistically significant volume element (1000 particles, say) in the steep concentration and potential gradients and high fluxes (i.e. nonequilibrium state) in the films. A concentration of 10^{-7} moles means on average one in every 400 volume elements contains one ion, below which the Nernst equation may not be valid [18]. This casts doubt on the numerical value calculated for the diluate concentration at the membrane face, but there is no doubt that the true concentration must be extremely low.

5.2. *Back e.m.f. and concentration boundary layer δ*

Figure 5 shows the effect of increasing the applied voltage under constant hydrodynamic conditions.

Insignificant polarization yields a negligible back e.m.f., such that the potential across the module drops to the bulk concentration-generated value, the value predicted from Equation 2, within 1.25 ms of zeroing the applied voltage. According to Fig. 5, the limiting applied voltage under the operating conditions employed occurs between 17 and 22 V. This is in reasonable agreement with the proposed limiting voltage of around 1 V per cell pair [1], below which polarization is not significant.

The plateaux evident at applied potentials above ≈ 23 V represent the relaxation time τ. Increasing the applied voltage increases E_b, as represented by the height of the plateau on curves 4–6, proportionally

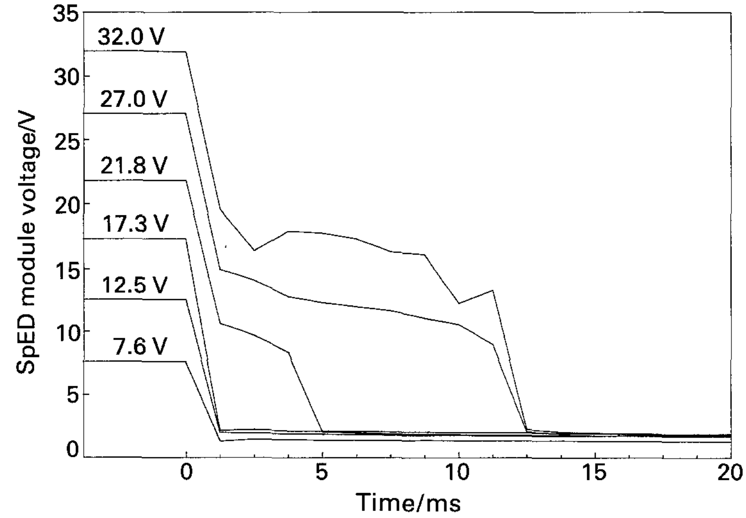

Fig. 5. Voltage (depolarization) transients for several applied voltage values. Operating parameters given in Tables 1 and 2.

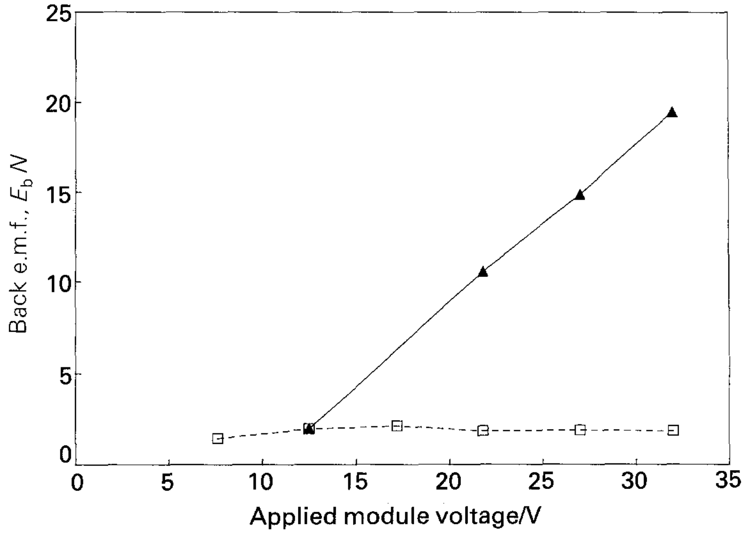

Fig. 6. Back e.m.f. against applied voltage. Operating parameters given in Tables 1 and 2. Key: (—) Polarization, (---) no polarization.

(Fig. 6). Above an applied voltage of about 23 V, the relaxation time τ is near constant. An average τ value of 15.5 ms (± 3.6 ms) was obtained from three consecutive experiments carried out on the same module under identical operating conditions. According to Equation 8, this corresponds to a δ value of approximately 6 μm, assuming a value of 0.002 mm^2 s^{-1} for the diffusion coefficient D [2]. This δ value is somewhat lower than values calculated from I_{lim} data using Equation 3: 10 μm has been measured for a planar electrode in contact with a rapidly-stirred solution [20], and a value of 9 μm quoted by Cooke [2] for a similar system. δ would be expected to decrease further with increasing velocity. No attempt was made to alter the system hydrodynamics during the current trials, and the effect of the diluate flow rate on τ has yet to be studied.

5.3. *Potential transient*

It has been assumed that the potential decay transients due to depolarization shown in Figs 4 and 5 are indicative of a rapid decrease in the surface concentration on the diluate side as t approaches τ. In fact, whilst there is evidence to support this postulation, there are two evident inconsistencies:

1. If a linear decrease in the surface concentration with time is assumed [2], then

$$\frac{C_1^*}{C_1} = \frac{t}{\tau} \tag{9}$$

The expected form of the potential transient, from Equation 3, is then

$$E_b = 0.118N \log(C\tau/t) + E_{be} \quad \text{at } 0 < t < \tau \tag{10}$$

where N is the number of cell pairs where polarization occurs, C is the concentration ratio C_2/C_1, E_{be} is the equilibrium back e.m.f. given by Equation 2. This is in marked contrast with the experimentally-derived relationship, which appears to approximate to the form:

$$E_b = k_1 \log((\tau - 1)/\tau) + E_{b0} \quad \text{at } 0 < t < 0.9\tau \tag{11}$$

where k_1 is an empirically derived constant, E_{b0} is the initial back e.m.f. given by Equation 3.

Plots of Equations 10 and 11 are given in Fig. 7.

2. The relaxation time would be expected to be independent of the applied voltage at all values of the latter above which complete polarization takes place.

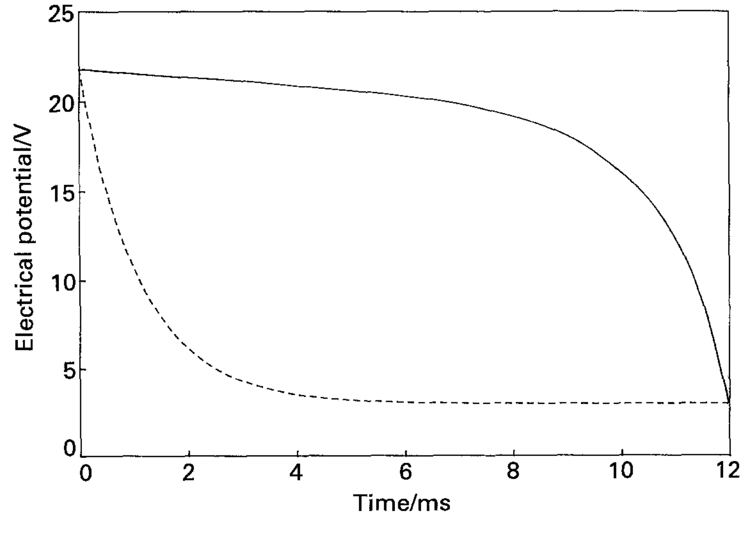

Fig. 7. Nernstian and experimentally-derived depolarization curves, Equations 10 and 11, respectively. Key: (---) Predicted, (—) measured.

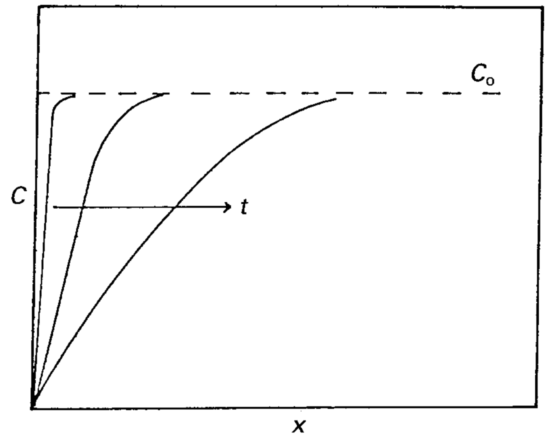

Fig. 8. Concentration transients derived from Equation 12, (taken from [21]).

The anomolously low value of τ obtained at $V = 23\,\mathrm{V}$ can be attributed to incomplete polarization at one or both membranes. Partial polarization results from the heterogeneity of the membrane surfaces.

The nonlinear form of the potential transient suggests that rate of change of the surface concentration of the diluate is not constant, but rather increases with time. Transient concentration profiles for interfacial polarization following a potential step are derived from the error function, are depicted in Fig. 8 [21]. The error function describes the interfacial concentration profile transient under stagnant fluid conditions, which for a normal potential step experiment is given by [19, 21]:

$$C(x, \mathbf{t}) = C_0 \operatorname{erf}\left(\frac{x}{2(D\mathbf{t})^{1/2}}\right) \qquad (12)$$

where $\mathbf{t}$ is the elapsed time after applying the potential and C_0 is the bulk (diluate) concentration (C_1). If it can be assumed that transient concentration profiles for depolarization follow the same function as that given in Equation 12, then, in this case

$$\mathbf{t} = \tau - t \qquad (13)$$

According to Equations 12 and 13, depolarization in the semistagnant liquid layer can take place without any change in the surface concentration until $t = \tau$. This would seem to describe the observed experimental trend with reasonable accuracy.

δ can be derived by integration of Equation 12 under similar boundary conditions to those employed in deriving Equation 7 to give [19]:

$$\delta = (\pi D \tau)^{1/2} \qquad (14)$$

Equation 14 yields an average value of $10.5\,\mu\mathrm{m}$ for δ from the experimentally-measured relaxation time. This value is in good agreement with previously reported δ values [2, 20].

A factor affecting the interfacial concentration profile is the velocity distribution. The idealized Nernst model of boundary layers assumes complete mixing of the solution in the centre of the flow channels and a sharp line of demarcation between completely mixed bulk solution and the stagnant solution in boundary layers adjacent to the membrane surface. This is recognized as being an oversimplification. A more realistic representation is a series of liquid layers undergoing laminar flow, with the liquid layer velocity increasing with increasing distance from the membrane surface [19]. Ion transport by convection would be promoted at the higher liquid velocities away from the membrane surface, yielding transient concentration profiles similar to those shown in Fig. 8.

6. Conclusion

A novel method for measuring the potential due to concentration polarization in an electrodialysis apparatus has been developed. Experimental evidence suggests that this potential becomes the dominant factor in determining that operational efficiency when concentration polarization is significant. The back e.m.f. increases linearly with applied voltage when the limiting current is exceeded.

The technique is quick, simple and reliable. It gives a direct measurement of the degree of polarization and permits rough calculation of the actual membrane surface concentration. It may find further application in the measurement of boundary film thickness in other membrane apparatus.

It is hoped that further work using the technique will establish the validity of the proposed relationship between the recorded relaxation time for depolarization and the thickness of the concentration boundary layer.

Acknowledgement

This work was funded by the Process Engineering Committee of the Science and Engineering Research Council.

References

[1] G. Solt, Electrodialysis, *in* 'Membrane Separation Process', (edited by P. Meares) Elsevier, Amsterdam (1976) Chapter 6.
[2] B. A. Cooke, *Electrochim. Acta* **3** (1961) 307–317.
[3] B. A. Cooke and S. J. Van der Walt, *Electrochim. Acta* **5** (1961) 216–218.
[4] W. G. B. Mandaersloot and R. E. Hicks, *IEC Proc. Des. Dev.* **4**(3), (1965) 304–308.
[5] K. S. Spiegler, Electrochemical operations, *in* 'Ion Exchange Technology' (edited by F. C. Nachod and J. Schubert) Academic Press, New York (1956) Chapter 6.
[6] V. K. Indusekhar and P. Meares, 'Physicochemical Hydrodynamics', (edited by D. B. Spalding) Adv. Publish Ltd, London (1977), **2**, pp. 1013–1043.
[7] R. Passino, G. Boari, A. Rozzi and G. Tiravanti, *Desalination* **24** (1978) 55–82.
[8] G. Tiravanti and R. Passino, *J. Membrane Sci.* **13** (1983) 349–363.
[9] G. Tiravanti, *ibid.* **9** (1981) 229–243.
[10] T. Yoshinobu, *ibid.* **57** (1991) 217–235.
[11] T. V. Arden and G. Solt, *British Patent 759 275.*
[12] G. Solt and T. Wen, *IChemE Sym. Ser.* **127** (1992) 11–22.
[13] *Idem.* paper presented at conference: 'Engineering of Membrane Process' at Bavaria, Germany (May 1992).

[14] P. Feron, 'Hydrodynamics and Mass Transfer in Obstructed Narrow Channels', PhD thesis, Cranfield Institute of Technology, UK (1991).

[15] G. Manecke, *Z. Physik. Chem.* **201** (1952) 1–15.

[16] J. N. Weinstein and F. B. Leitz, *Science* **191** (1976) 557–559.

[17] J. N. Bronsted *in* 'International Critical Tables', Volume IV, McGraw-Hill, London (1929) p. 216.

[18] P. Meares, private communication (1992).

[19] Zha Quan-Xing, 'Kinetics of Electrode Processes', Science Press, Beijing (1987), pp. 89–121.

[20] D. R. Crow, 'Principles of Electrochemistry', 3rd edn., Chapman & Hall, London (1991) p. 178.

[21] D. D. MacDonald, 'Transient Techniques in Electrochemistry', Plenum, New York/London (1977) p. 72.